JOURNAL OF THE AMERICAN WATER RESOURCES ASSOCIATION
Vol. 47, No. 1 AMERICAN WATER RESOURCES ASSOCIATION February 2011

SIMULATED IMPACTS OF THREE DECADAL CLIMATE VARIABILITY PHENOMENA ON WATER YIELDS IN THE MISSOURI RIVER BASIN[1]

Vikram M. Mehta, Norman J. Rosenberg, and Katherin Mendoza[2]

ABSTRACT: The Missouri River Basin (MRB) is the largest river basin in the United States (U.S.), and is one of the most important crop and livestock-producing regions in the world. In a previous study of associations between decadal climate variability (DCV) phenomena and hydro-meteorological (HM) variability in the MRB, it was found that positive and negative phases of the Pacific Decadal Oscillation (PDO), the tropical Atlantic sea-surface temperature gradient variability (TAG), and the west Pacific warm pool (WPWP) temperature variability were significantly associated with decadal variability in precipitation and 2-meter air temperature in the MRB, with combinations of various phases of these DCV phenomena associated with drought, flood, or neutral HM conditions. Here, we report on a methodology developed and applied to assess whether the aforementioned DCVs directly affect the hydrology of the MRB. The Hydrologic Unit Model of the U.S. (HUMUS) was used to simulate water yields in response to realistic values of the PDO, TAG, and WPWP at 75 widely distributed, eight-digit hydrologic unit areas within the MRB. HUMUS driven by HM anomalies in both the positive and negative phases of the PDO and TAG resulted in major impacts on water yields, as much as ±20% of average water yield in some locations. Impacts of the WPWP were smaller. The combined and cumulative effects of these DCV phenomena on the MRB HM and water availability can be dramatic with important consequences for the MRB.

(KEY TERMS: irrigation; climate variability/change; drought; precipitation; streamflow; simulation; rivers/streams.)

Mehta, Vikram M., Norman J. Rosenberg, and Katherin Mendoza, 2011. Simulated Impacts of Three Decadal Climate Variability Phenomena on Water Yields in the Missouri River Basin. *Journal of the American Water Resources Association* (JAWRA) 47(1):126-135. DOI: 10.1111/j.1752-1688.2010.00496.x

INTRODUCTION

Interannual to Decadal Climate Variability

The El Niño-Southern Oscillation (ENSO; see Table 1 for a list of abbreviations used in this paper) phenomenon in the tropical Pacific and its impacts on United States (U.S.) climate are well known (see, e.g., Ropelewski and Halpert (1986), Rasmusson (1991)). It is also well known that ENSO frequency and intensity undergo decadal and longer time-scale variability (Gu and Philander, 1995; Kestin *et al.*, 1998; Torrence and Webster, 1999). Also, impacts of ENSO on global climate appear to vary at decadal and longer time scales (Mehta and Lau, 1997;

[1]Paper No. JAWRA-10-0017-P of the *Journal of the American Water Resources Association* (JAWRA). Received February 12, 2010; accepted September 26, 2010.
[2]Respectively, Executive Director, Senior Scientist, and Research Assistant, Center for Research on the Changing Earth System, P.O. Box 346, Clarksville, Maryland 21029 (E-Mail/Mehta: vikram@crces.org).

TABLE 1. Abbreviations.

DCV	Decadal climate variability
ENSO	El Niño-Southern Oscillation
GIS	Geographic information system
HM	Hydro-meteorological
HUMUS	Hydrologic Unit Model of the U.S.
MEI	Multivariate ENSO Index
MRB	Missouri River Basin
MWRR	Major Water Resource Region
NAO	North Atlantic Oscillation
PDO	Pacific Decadal Oscillation
SST	Sea-surface temperature
SWAT	Soil and Water Assessment Tool
TAG	Tropical Atlantic Gradient
USDA	U.S. Department of Agriculture
USGS	U.S. Geological Survey
WPWP	West Pacific warm pool

McCabe and Dettinger, 1999; Power *et al.*, 1999; Torrence and Webster, 1999; Arblaster *et al.*, 2002). Now, in addition, a group of decadal ocean-atmosphere phenomena, such as variability of the west Pacific warm pool (WPWP) temperature (Wang and Mehta, 2008), the tropical Atlantic sea-surface temperature (SST) gradient (Hastenrath, 1990; Houghton and Tourre, 1992; Mehta and Delworth, 1995; Mehta, 1998; Rajagopalan *et al.*, 1998), the subtropical-midlatitude Pacific climate variability generally known as the Pacific Decadal Oscillation (PDO) (Mantua *et al.*, 1997), and their impacts on the U.S. climate are attracting increasing attention.

Importance of the Missouri River Basin

The Missouri River Basin (MRB) is the largest river basin in the U.S., covering more than 500,000 square miles and including all or parts of 10 states (Montana, Wyoming, Colorado, North Dakota, South Dakota, Minnesota, Iowa, Nebraska, Kansas, and Missouri), numerous Native American reservations, and small portions of the Canadian provinces of Alberta and Saskatchewan. The population of the MRB depends on the Missouri River for drinking water, irrigation and industrial needs, hydroelectricity, recreation, navigation, and fish and wildlife habitat. The MRB contains some of the country's most sparsely populated agrarian counties as well as a number of important metropolitan areas such as Omaha and Kansas City on the Missouri River and Denver at the foothills of the Rocky Mountains (see, e.g., Rosenberg, 2007). The Missouri River drains much of the eastern slopes of the Rocky Mountains; most of the Great Plains region; and western portions of the prairie states of Minnesota, Iowa, and Missouri.

Grain crops for food and feed provide much of the MRB's agricultural income. The MRB is a very important food-producing region not only of the U.S. but also of the world. The MRB produces approximately 46% of U.S. wheat, 22% of its grain corn, and 34% of its cattle. About 117 million acres (~47.35 million ha) are in cropland in the aforementioned states. Of that total, about 12 million acres (~4.86 million ha) are irrigated. Thus, agricultural production in almost 90% of the MRB's cropland is entirely dependent on precipitation.

Of the 18 Major Water Resource Regions (MWRRs) of the conterminous U.S., freshwater withdrawals for irrigation are greatest in California, the Pacific Northwest, and the MRB. Gleick (1990) characterized the vulnerability of these 18 MWRRs to climate change by reference to five indicators; these are measures of *storage capacity*, *demand*, *dependence on hydroelectricity*, *groundwater vulnerability*, and *streamflow variability*. California and the MRB were vulnerable on four indicators; only their *storage capacity* was (as of 1990) deemed adequate. The vulnerability of the MRB fluctuates, of course, with precipitation variability forced by large-scale climate variability, especially at interannual and decadal time scales, which, as mentioned below, explains 60-70% of the total variance of annual-average precipitation. For example, during a major, multiyear-to-decadal (hereafter referred to as decadal) drought such as that in the 1950s and the late 1980s inflows in the MRB were insufficient to fully support reservoir-based recreation and Missouri River navigation (see, e.g., Murray, 2005). This was true as well during the recent drought from 2000-2001 to late spring 2008. Conversely, too much water in the MRB reservoir system during above-average precipitation years requires greater water releases from the reservoirs, sometimes threatening the viability of farming and integrity of home sites in the MRB floodplain. In spite of the estimated adequate storage capacity in the MRB to cope with climate change on a long-term average basis, decadal droughts in the MRB deplete the stored water to the extent that tensions flare up between holders of senior and junior water rights, and between upstream and downstream states. In such a situation, an equitable distribution of the MRB water becomes a matter of national concern (Murray, 2005).

Decadal Climate Variability in the Missouri River Basin

In addition to ENSO-related precipitation variability in the Great Plains and the Midwest, there are indications that other large-scale climate forcings by

the PDO (Ting and Wang, 1997; Smith *et al.*, 1999), the North Atlantic Oscillation (NAO) (Hurrell *et al.*, 2001), and the WPWP variability (Wang and Mehta, 2008) also influence precipitation variability in the Great Plains. More specifically in the MRB, Cayan *et al.* (1998) found that interannual ENSO variability explains <20% and decadal time-scale variability explains approximately 40-50% of the total precipitation variance. Cayan *et al.* (1998) also found that snow accumulation and stream discharge variations in the MRB generally agree with the interannual and decadal precipitation variability estimates. These results are consistent with runoff and streamflow analyses by Guetter and Georgakakos (1993) and Lins (1997). These precipitation, snow accumulation, and stream discharge estimates are also reflected in the percentage area of the MRB under severe-to-extreme drought conditions; the fraction of the MRB experiencing severe-to-extreme drought in the 20th Century has ranged from 20% to 60% or more at interannual to decadal time scales (http://drought.unl.edu/whatis/palmer/riverbasin.htm).

Recently, V.M. Mehta, K. Mendoza, and N.J. Rosenberg (manuscript in preparation) conducted analyses of associations between tropical-subtropical decadal climate variability (DCV) phenomena and hydro-meteorological (HM) variability in the MRB for Northern Hemisphere spring and summer, the main growing seasons in the MRB. Indices of ENSO (Multivariate ENSO Index, MEI), PDO, WPWP variability, and tropical Atlantic SST gradient (TAG for brevity) variability from 1950 to 1999 were used in these analyses. HM observations consisting of monthly precipitation rate, 2-meter air temperature, 2-meter wind speed, and relative humidity from 1950 to 1999 were assembled and used in this analysis as were streamflow observations from the U.S. Geological Survey. It was found that PDO, TAG, and WPWP are associated significantly with decadal precipitation and 2-meter air temperature variability in the MRB, with combinations of various phases of these DCV phenomena associated with drought, flood, or neutral HM conditions.

Three extreme hydrologic events in the MRB – droughts in the mid-1950s and the mid- to late 1980s, and floods in the early to mid-1990s – were reconstructed using results of these statistical analyses. The 1950s drought event was found to be associated primarily with the negative phase of the PDO and the 1980s drought event was found to be associated primarily with the negative phase of the TAG. The 1990s flood event was found to be associated with coincident positive phases of both the TAG and the PDO. The WPWP variability also contributed to these and other hydrologic excursions in the MRB. Thus, V.M. Mehta, K. Mendoza, and N.J. Rosenberg (manuscript in preparation) found that, rather than one DCV phenomenon being responsible for every occurrence of drought or flood/wet period, combinations of phases of multiple DCV phenomena can be linked with large and persistent hydrologic events in the MRB.

In a first attempt to develop methodology suitable for analyzing the role of DCVs in HM variability and its impacts within the MRB and in recognition of the foregoing, we undertook an exploratory, systematic, and multidisciplinary assessment of impacts of the three aforementioned DCV phenomena on water resources in the MRB. In this study, we employed the Hydrologic Unit Model of the U.S. (HUMUS) system (Srinivasan *et al.*, 1993 as recently employed by Thomson *et al*., 2005a,b,c) to simulate DCV impacts on water yields, along with the HM data used in the V.M. Mehta, K. Mendoza, and N.J. Rosenberg (manuscript in preparation) study and U.S. Geological Survey (USGS) streamflow data. Here, we report the simulated impacts of three individual DCV phenomena – PDO, WPWP variability, and TAG variability – on water yields in the MRB. A similar study to simulate effects of various types of El Niño events on North American water resources by Thomson *et al.* (2003) also used the HUMUS system.

The HUMUS model, its parameterizations and calibration against USGS streamflow data, and the experimental design are described in the next section. Then, the validation of historic water yields simulated by HUMUS and impacts of hypothetical DCV scenarios on water yields are described. Finally, results are discussed and conclusions are presented.

THE HYDROLOGIC UNIT MODEL OF THE U.S. SYSTEM AND EXPERIMENT DESIGN

Description of Soil and Water Assessment Tool and Hydrologic Unit Model of the U.S.

The HUMUS (Srinivasan *et al.*, 1993) is a geographic information system (GIS)-based modeling system that provides input to the Soil and Water Assessment Tool (SWAT) (Arnold and Allen, 1992; Arnold *et al.*, 1998) at the subbasin scale and aggregates the output into larger basins. The HUMUS can be applied to a wide range of basin sizes depending on the availability of required input data. In this study, 25 of the 30 four-digit USGS hydrologic unit areas (USGS, 1987) in the MRB were selected for sampling. Three eight-digit subbasins represented by nearby climatological stations were selected in each of the 25 four-digit basins for a total of 75 study sites. Climate

and soil type were treated as uniform within each of the 75 subbasins. It was also assumed that the current, dominant land use in the basin applies to its entirety.

The SWAT represents the basin water balance through four storage volumes: snow, soil profile (0-2 m), shallow aquifer (0-20 m), and deep aquifer (>20 m). Biophysical and hydrological processes simulated by SWAT include the net primary productivity of the vegetative cover, infiltration, potential and actual evapotranspiration, lateral flow, and percolation. SWAT calculates water yield (the variable most comparable with streamflow) as the sum of surface and lateral flow from the soil profile and groundwater flow from the shallow aquifer.

The HUMUS system works on a daily time step using daily values of precipitation, maximum and minimum temperatures, relative humidity, and wind speed. Weather data can be drawn from historic records for retrospective or synoptic studies or, where the data are inadequate, weather data generators can be used to synthesize the necessary input data for SWAT. The WXGEN weather generator of Richardson and Nicks (1990) is integrated into SWAT for this purpose. For prospective studies of climate change, SWAT includes algorithms to simulate the "fertilization effect" of rising atmospheric CO_2 concentrations on photosynthesis for C3 plants (legumes, small grains, cool season grasses, and most trees) and increased stomatal resistance to transpiration for both C3 and C4 plants (tropical grasses such as corn, sorghum, millet, sugar cane, and other warm-season grasses) (Stockle *et al*., 1992a,b). As the CO_2-fertilization effect was not a consideration in the study reported here, a constant and uniform concentration of CO_2 of 330 parts per million by volume was used in the simulations.

Calibration and Validation of Hydrologic Unit Model of the U.S.

The SWAT/HUMUS system has been validated with observed data at scales ranging from the MWRR (Arnold *et al.*, 1999) to a small stream catchment (Arnold and Allen, 1996). Gerbert *et al.* (1987) estimated the annual-average natural streamflow from observations at approximately 6,000 gauging stations in the U.S. over the period 1951 to 1980. Arnold *et al.* (1999) found that HUMUS agreed reasonably well with the Gerbert *et al.* (hereafter, USGS-estimated) streamflow with regression slopes of 0.86 at the state level and 1.01 at the level of STATSGO soil association regions. (STATSGO is a GIS-accessible soils database developed by the USDA/Natural Resources Conservation Service). In a contribution to the study "Climate Change Impacts on the U.S: The Potential Consequences of Climate Variability and Change" (otherwise known as the National Assessment, OSTP, 2000), Rosenberg *et al.* (2003) found that HUMUS adequately represented streamflow over most of the conterminous U.S., but overestimated runoff in the Great Plains and the Mississippi Delta, probably an artifact of applying irrigation to all lands within each subbasin in which irrigation is practiced. They also found that HUMUS underestimated streamflow in mountainous regions, probably because of a lack of weather observations from high-altitude locations. Thomson *et al.* (2005a,b) also validated HUMUS in a study of the entire conterminous U.S. of hydrologic sensitivity to a set of three climate change scenarios derived from three general circulation models.

Further evidence of the utility and validity of the SWAT/HUMUS system was shown in the report of their "National Assessment" work in Rosenberg *et al.* (2003). Simulated annual water yield, the independent variable, was correlated with USGS-observed water yield, at the outlet of each of the 18 USGS MWRRs in the conterminous U.S., the dependent variable, is shown in Figure 2 (p. 79) of Rosenberg *et al.* (2003); a regression slope of 0.88 is shown with an R^2-value of 0.92 for the MRB.

Another fact supporting the use of the SWAT/HUMUS in the current application is its relatively good agreement on overall annual water yield in the MRB. Drawn from different sources and different periods of record, these estimates are 56 mm/year (Mather, 1984) and 64 mm/year (Waggoner and Shefter, 1990) (summarized in Table 1, p. 77, of Rosenberg *et al.*, 2003). The SWAT/HUMUS-simulated average water yield for the MRB reported in Rosenberg *et al.* (2003) was 94 mm/year. USGS measurements (again for a different time period) was 74 mm/year.

Preparation of Base Climatology and Decadal Climate Variability Scenarios

Following a satisfactory validation of simulated and USGS water yield anomalies for test locations across the MRB, the next step was to increase the number of locations to be used in further simulations across the basin. The HM variables (HMVs) used for the period 1950-1999 were from Maurer *et al.* (2002) and consist of the daily precipitation rate, 2-meter maximum and minimum air temperature, 2-meter wind speed, and 2-meter relative humidity. This dataset is available for North America at a resolution of 1/8° longitude – 1/8° latitude from www.jisao.washington.edu/data/vic. A daily data series for each of the five HMVs was obtained as an area-average of nine (3×3) grid points representing each location. This was done for three eight-digit basins in each of

TABLE 2. Combination of Amplitudes and Phases of DCV Phenomena in Each Scenario.

DCV Phenomenon	Positive Phase	Negative Phase
PDO	+0.75	−0.75
TAG	+0.3	−0.3
WPWP	+0.1	−0.1

the 25 (out of 30) four-digit basins within the MRB (totaling 75 locations in all). The five four-digit basins omitted from this study are located in mountainous regions of Montana, where climate stations are few in number more or less unsuitable for dryland farming.

The monthly statistics at each of the 75 locations were created by averaging daily data over a 10-year period from 1990 to 1999 so as to simulate DCV impacts with respect to the most recent 10-year climatology available from this dataset. These served as the base climatology for the creation of the DCV-related weather scenarios. As our interest in this research is primarily in studying the sensitivity of water yields to DCV phenomena, we filtered all monthly HMVs and DCV indices for the 1950 to 1999 period with a low-pass filter that allowed periods equal to or longer than eight years to pass through without any attenuation of amplitude and removed all periods shorter than eight years. In order to generate DCV-related weather scenarios using the low-pass filtered data, regression analysis was carried out for each of the five filtered, monthly HMVs with filtered, monthly PDO, WPWP, and TAG indices. The corresponding regression slopes were then multiplied by average positive and average negative values of each DCV index during the 1950 to 1999 period. An annual cycle of each of the six DCV-related scenarios, realistic in amplitude and positive or negative in phase, was created. To complete each DCV-related weather scenario, the annual cycle of monthly HMV anomalies corresponding to each of the six DCV scenarios was then added to the corresponding monthly average climatology values. The amplitude and phase of each of the DCV scenarios are shown in Table 2. A simulation experiment for each scenario was run with HUMUS forced by monthly HMVs for each scenario repeated for 10 years. The total monthly HMVs were provided as an input to the weather generator in HUMUS whose daily output was provided as an input to the SWAT part of HUMUS. Thus, we obtained 10 annual samples of water yields and other hydrologic variables for each scenario. Results averaged over the 10 samples are described in this paper. Results were analyzed both at individual locations and for the entire MRB as one location.

IMPACTS OF INDIVIDUAL DECADAL CLIMATE VARIABILITY SCENARIOS ON WATER YIELD

Hydro-meteorological Anomalies Associated With the Three Decadal Climate Variability Phenomena

As described in the previous section, low-pass filtered HMV anomalies were individually regressed against each low-pass filtered DCV index (PDO, TAG, and WPWP) for each month using data from 1950 to 1999. Regression coefficients were then used to estimate HMV anomalies for each month for specified values of an individual DCV index. Simultaneous correlation coefficients among the three DCV indices were negligible. HMV anomalies at each location where HUMUS runs were made are described in this section.

Regression analysis showed that substantial precipitation and temperature anomalies in the MRB were associated with both phases of the PDO as shown in Figure 1. Figure 1a shows that precipitation anomalies associated with PDO^+ (positive phase of the PDO) were generally positive in the entire MRB, except in the northwest part of the basin where they were negative. Figure 1d shows that precipitation

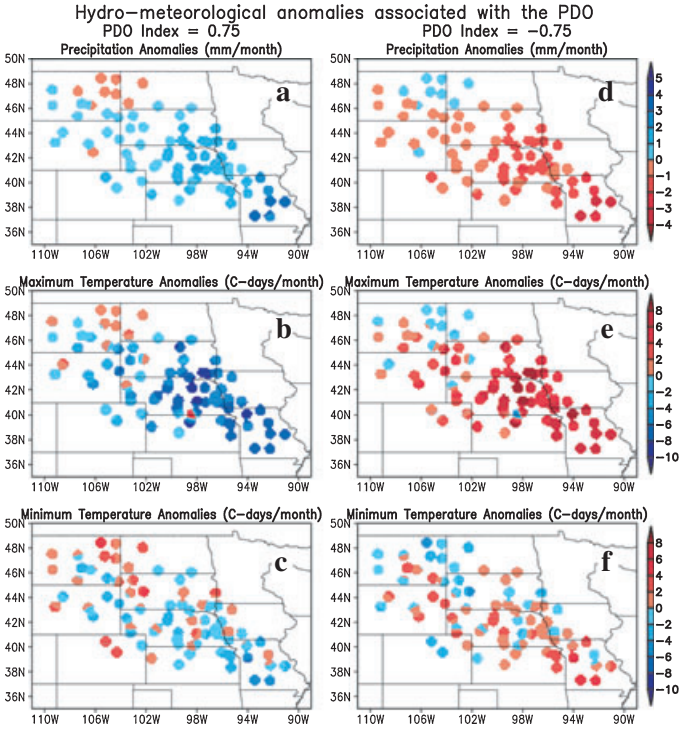

FIGURE 1. Hydro-meteorological Anomalies Associated With (a,d respectively) PDO^+ and PDO^- Precipitation (mm/month), (b,e) Daily Maximum Temperature (°C-days/month), and (c,f) Daily Minimum Temperature (°C-days/month).

anomalies associated with PDO$^-$ (negative phase of the PDO) were generally negative, except in the northwest part of the basin where there were a few locations with positive anomalies. Largest precipitation anomalies associated with the PDO ranged from 3 to 5 mm/month in PDO$^+$ to −3 to −4 mm/month in PDO$^-$. During PDO$^+$, as shown in Figure 1a, precipitation was above-average almost everywhere in the MRB; daily maximum temperature (T_{max} hereafter; Figure 1b) was below average except in western Wyoming, Montana, and western North Dakota; and daily minimum temperature (T_{min} hereafter; Figure 1c) was below average along a northwest-southeast axis from southeast Montana to southern Iowa, and above-average southwest and northeast of this axis. In PDO$^-$, precipitation (Figure 1d) was below average in the eastern half of the MRB; in Montana and western North Dakota, precipitation was below average but not as much as under PDO$^+$, and there were a few locations where precipitation was above average except in Montana and western North Dakota where it was below average. T_{max} (Figure 1e) was above average in the PDO$^-$ phase almost everywhere in the basin. T_{min} (Figure 1f) was also above average in the PDO$^-$ phase almost everywhere in the MRB except in Montana and western North Dakota where it was below average.

In the TAG$^+$ phase (Figure 2), precipitation was below average almost everywhere in the MRB. Associated with these precipitation changes were T_{max} increases of approximately 0 to 4°C-days/month almost everywhere in the MRB (Figure 2b), except at a few locations in central South Dakota, northern Wyoming, Nebraska, Kansas, and northeast Colorado where T_{max} decreased by a few °C-days/month. Except for a few locations, especially in the western part of the MRB, T_{min} was generally below average (Figure 2c). In the TAG$^-$ phase, precipitation (Figure 2d) increased approximately 1 to 3 mm/month everywhere except at a few locations in South Dakota and Nebraska. T_{max} was generally below average everywhere ranging from approximately 2 to 6°C-days/month (Figure 2e). T_{min} was above average approximately 0 to 4°C-days/month in the eastern half of the MRB, and below average approximately −2 to −4°C-days/month in Colorado, western Nebraska, and Wyoming (Figure 2f).

Precipitation anomalies tended to be less dramatic than under PDO or TAG and were generally of opposite signs in WPWP$^+$ and WPWP$^-$ phases. In southeastern MRB (Missouri, southwestern Iowa), precipitation anomalies were −1 to −2 mm/month in WPWP$^+$ (Figure 3a) and 0 to 2 mm/month in WPWP$^-$ (Figure 3d). In central MRB (Nebraska, northern Kansas), precipitation anomalies were 0 to 2 mm/month in WPWP$^+$ and 0 to −2 mm/month in WPWP$^-$.

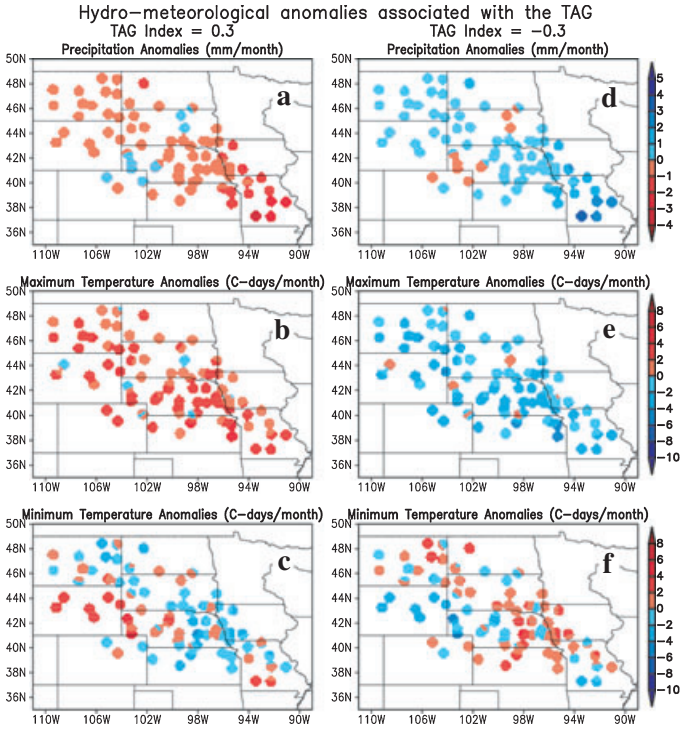

FIGURE 2. Hydro-meteorological Anomalies Associated With (a,d respectively) TAG$^+$ and TAG$^-$ Precipitation (mm/month), (b,e) Daily Maximum Temperature (°C-days/month), and (c,f) Daily Minimum Temperature (°C-days/month).

In northwestern MRB (western South Dakota, North Dakota, Wyoming, Montana), precipitation anomalies were largely negative (0 to −2 mm/month) in WPWP$^+$ and 0 to 2 mm/month in WPWP$^-$. T_{max} anomalies were up to 1 to 4°C-days/month in WPWP$^+$ (Figure 3b) and −1 to −4°C-days/month in WPWP$^-$ (Figure 3e). T_{min} anomalies were also up to 4°C-days/month in WPWP$^+$ (Figure 3c), but below average by as much as −6°C-days/month in WPWP$^-$ (Figure 3f).

Impacts on Water Yield

As described in section "Calibration and Validation of Hydrologic Unit Model of the U.S." and "Preparation of Base Climatology and Decadal Climate Variability Scenarios," HUMUS was calibrated and validated for the MRB in previous studies. For comparison with impacts of the DCV scenarios on water yield, the average water yield simulated by HUMUS for the 1990 to 1999 period is shown in Figure 4. The simulated water yield was maximum (200 to more than 350 mm/year) in Missouri, southwest Iowa, and east Kansas, and generally decreased toward northwest MRB to <50 mm/year.

In response to HMV anomalies associated with PDO$^+$ (Figures 1a, 1b, and 1c), water yield (Figure 5a)

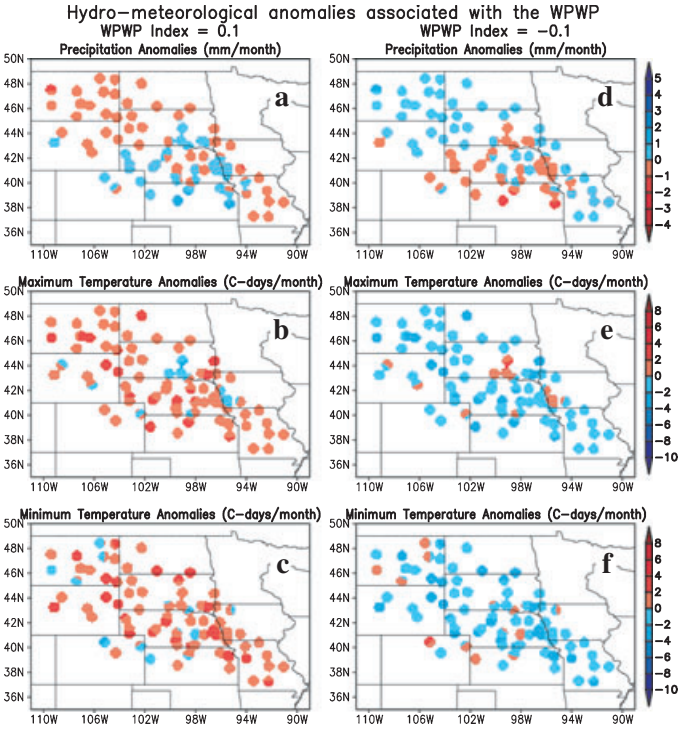

FIGURE 3. Hydro-meteorological Anomalies Associated With (a,d respectively) WPWP$^+$ and WPWP$^-$ Precipitation (mm/month), (b,e) Daily Maximum Temperature (°C-days/month), and (c,f) Daily Minimum Temperature (°C-days/month).

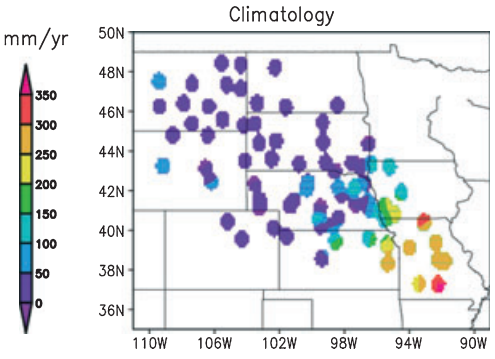

FIGURE 4. Simulated Average Water Yield During 1990-1999.

increased by 10-40% of average yield (Figure 4) in much of the MRB, except in eastern Montana, western North Dakota, and individual locations in Nebraska and Wyoming where the yield decreased by 10-30%. In response to HMV anomalies associated with PDO$^-$ (Figures 1d, 1e, and 1f), water yield (Figure 5b) decreased almost everywhere by 10-30%, except in individual locations in Montana, North and South Dakota, Wyoming, Kansas, and Missouri. The average yield change over the entire MRB in the PDO$^+$ and PDO$^-$ phases was within ±20% of average yield.

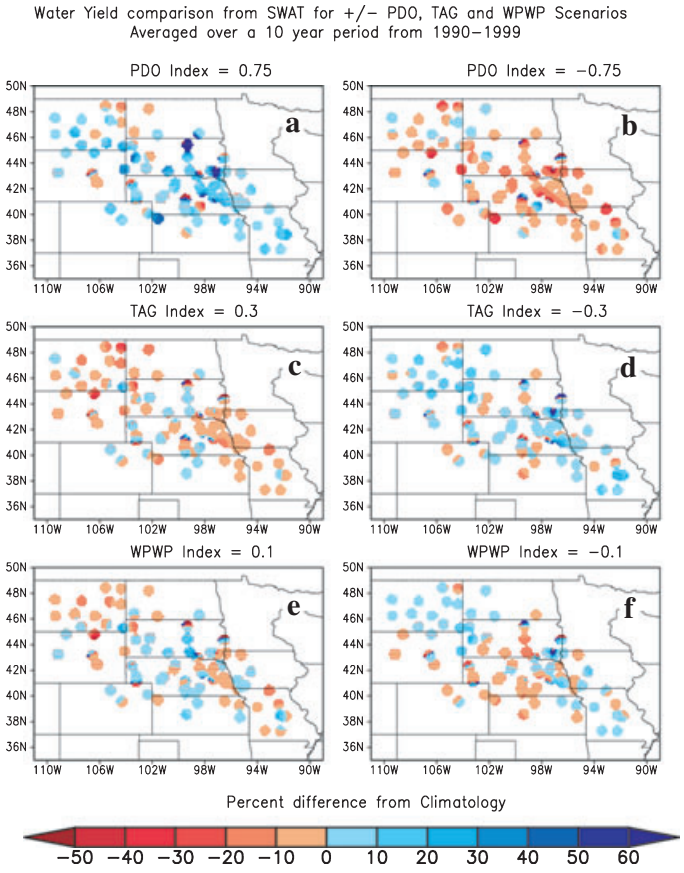

FIGURE 5. Simulated Water Yield Anomalies (%) in the MRB: (a) PDO$^+$, (b) PDO$^-$, (c) TAG$^+$, (d) TAG$^-$, (e) WPWP$^+$, and (f) WPWP$^-$. See text for more details.

In response to HMV anomalies associated with TAG$^+$ (Figures 2a, 2b, and 2c), water yield (Figure 5c) decreased almost everywhere in the MRB by 5-20%. In the central MRB (Kansas, Nebraska, and South Dakota) and at individual locations in Colorado and Montana, water yield increased by approximately 5-15%. In response to HMV anomalies associated with TAG$^-$ (Figures 2d, 2e, and 2f), water yield (Figure 5d) increased almost everywhere by approximately 5-20% with a few outliers near 30% in eastern South Dakota and Nebraska and with decreases of 5-10% at individual locations.

Figures 5e and 5f show water yield anomalies associated with WPWP$^+$ (Figures 3a, 3b, and 3c) and WPWP$^-$ (Figures 3d, 3e, and 3f) phases, respectively. As discussed earlier in this section, there were below-average precipitation and above-average temperatures in Missouri and western Iowa in WPWP$^+$, resulting generally in below-average water yield in this part of the MRB (Figure 5e). At the same time, there was below-average precipitation and above-average temperatures in the northwestern MRB (western North Dakota, western South Dakota, east-

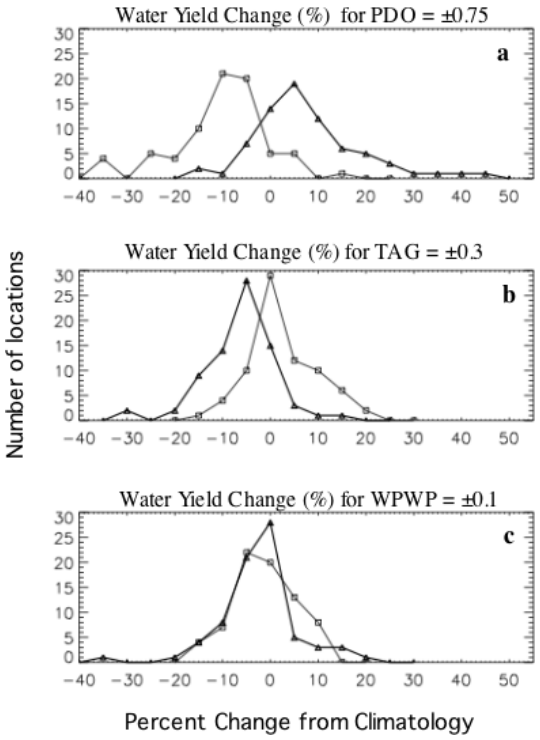

FIGURE 6. Aggregated Water Yield Anomalies (%) in the MRB: (a) PDO^+ and PDO^-; (b) TAG^+ and TAG^-; and (c) $WPWP^+$ and $WPWP^-$. Triangles denote positive phase and boxes denote negative phase. See text for more details.

ern Wyoming, and Montana), generally with above-average water yield. In Nebraska, there were both above- and below-average precipitation and above-average temperatures, and the water yield was 5-10% below average. The water yield response to HMV anomalies associated with $WPWP^-$ was generally opposite in sign to that in $WPWP^+$, which reflected generally opposite signs of precipitation and temperature anomalies in the two WPWP phases.

In order to estimate impacts of the three DCV phenomena on the MRB as a whole, binned distributions, or histograms, of number of locations in water yield anomaly bins were plotted for each phase of the three DCV phenomena. For convenience of presentation, the histograms are shown as continuous distributions, but they are actually binned distributions. These histograms are shown in Figure 6. A test of significance of differences in the binned distributions corresponding to positive and negative phases of each DCV phenomenon was conducted. This test (Press *et al.*, 2001) is based on a chi-square statistic calculated from two binned distributions, which is then used to calculate the probability of the two binned distributions belonging to the same population. The two binned distributions are more significantly different the smaller the chi-square probability function. For all three DCV phenomena, the probabilities of the distributions corresponding to positive and negative phases belonging to the same population were very small (5.2×10^{-11} for PDO, 8.4×10^{-7} for TAG, and 0.21 for WPWP), implying that impacts of positive and negative phases of each DCV phenomenon were significantly different, with PDO and TAG much more so than WPWP.

Histograms of water yield anomalies in the two PDO phases are shown in Figure 6a. They are in agreement with the two-dimensional results in Figures 4a and 4b. Although gains and losses occurred in subregions, the above-average precipitation and below-average temperatures in PDO^+ led to a general increase in water yields, whereas water yields generally decreased in the PDO^- phase. The water yield difference between the peaks of the two histograms was approximately 20%.

Histograms of aggregated water yield anomalies for the entire MRB in the two TAG phases are shown in Figure 6b. They reflect aggregated effects of each TAG phase in the MRB, in agreement with the two-dimensional results. In TAG^+, water yields in the southeastern part decreased between 5 and 20% in a large number of locations, whereas water yields increased between 5 and 10% in individual locations throughout the MRB. In TAG^-, the water yield distribution was generally opposite; there were a large number of locations with yield increases in the 5-20% range, whereas the decreases in yields were generally confined to 5%. Figure 6b shows significant differences in the peaks of the two histograms as well as in their shapes.

Histograms of aggregated water yield anomalies for the entire MRB in the two WPWP phases are shown in Figure 6c. The histograms reflect two-dimensional distributions of water yield anomalies such that the above-average precipitation and below-average temperatures in $WPWP^-$ phase resulted in above-average water yield when aggregated over the entire MRB. These differences are reflected in the overall histograms as differences in the shapes of the two histograms rather than in their peak value, and are not as significant as the differences for PDO and TAG phases.

DISCUSSION AND CONCLUSIONS

The HUMUS system was used in this exploratory study to simulate water yields in the MRB in response to HM anomalies associated with three DCV phenomena – the PDO, the TAG variability, and the WPWP variability. Realistic amplitudes and positive and negative phases of these three DCVs

were used in the simulations. Major results of the simulation experiments are as follows:

- Development of a methodology sensitive enough to detect effects of DCV phenomena on water yields on the local (eight-digit basin) and regional (MWRR) scales.
- Hydro-meteorological anomalies associated with realistic values of the PDO and TAG indices, applied to HUMUS, led to substantial impacts on water yields; impacts of the WPWP variability were smaller.

Overall, water yields were clearly reflective of the changes in HMVs associated with the individual DCVs and their phases as the hydrologic cycle is driven by precipitation and evapotranspiration and the latter is determined by the temperature, humidity, and windiness of the air. Perfect agreement should not be expected, however, as topography, soil type, antecedent soil moisture condition, and vegetative cover are also controlling and all of the latter factors were treated as uniform over the entire area of the eight-digit basins chosen for modeling. Although outliers exist, HUMUS-simulated water yields were generally consistent with DCV anomalies in HMVs, both locally (eight-digit basin) and regionally (MRB) in this exploratory study.

Again, our results show that two of the three DCV phenomena considered in this study, if they occur singly and for a multiyear to decadal period, can significantly impact water yields in the MRB. As these DCV phenomena can, indeed, persist in one phase or another for years to a decade or longer and as the simultaneous correlation among them is negligibly small, their combined and cumulative effects on the MRB hydro-meteorology should sufficiently impact all water sectors in the region – transportation, hydropower generation, municipal and industrial needs, fish and wildlife habitat, recreation, and, not the least, irrigation. The MRB is a major "breadbasket" in which most food and feed are produced on unirrigated land. In periods of drought, agricultural production is reduced and the contribution of irrigated land to regional production can also be significantly reduced by shortages of surface water supplies. In periods of ample rainfall, the overall contribution of irrigation to regional production is less critical.

Because the three DCV phenomena, whose impacts on water yields were modeled in this study, and others also influence the climate and hydro-meteorology in other parts of the world, our methodology could usefully be applied to gain an understanding of their possible impacts on water yields in those regions. Also, if in the future, the evolution of major DCV phenomena can be forecast with some skill, it may be possible with HUMUS and other well-known hydrology models to forecast, for some cases and regions, their multiyear to decadal impacts on water yields. Although decadal climate predictions are not yet available and are likely to remain highly experimental for some years, work toward that goal is proceeding in several climate modeling and prediction groups around the world.

Increasing climatic and other environmental stresses on global food production and the growing demand for food supplies provide just one example of the importance of continued and focused research on DCV phenomena and their impacts. In another phase of this study, the methodologies developed here are applied to drive a crop production simulation model. That study, to be submitted to an appropriate journal, suggests that the incidences of DCVs in their average positive or negative phases can significantly decrease or increase food production in the MRB.

ACKNOWLEDGMENTS

This research was supported by NOAA-Climate Office-Sectoral Applications Research Program Grant NA06OAR43100681. Jimmy Williams, R. Srinivasan, and their colleagues at the Texas A&M University provided training and advice in the use of the HUMUS system; their help is gratefully acknowledged. The authors thank Todd Mitchell of University of Washington for his help in obtaining hydro-meteorological data.

LITERATURE CITED

Arblaster, J.M., G.A. Meehl, and A.M. Moore, 2002. Interdecadal Modulation of Australian Rainfall. Climate Dynamics 18:519-531.

Arnold, J.G. and P.M. Allen, 1992. A Comprehensive Surface-Groundwater Flow Model. Journal of Hydrology 142:47-69.

Arnold, J.G. and P.M. Allen, 1996. Estimating Hydrologic Budgets for Three Illinois Watersheds. Journal of Hydrology 176:57-77.

Arnold, J.G., R. Srinivasan, R.S. Muttiah, and P.M. Allen, 1999. Continental Scale Simulation of the Hydrologic Balance. Journal of American Water Resources Association 35:1037-1051.

Arnold, J.G., R. Srinivasin, R.S. Muttiah, and J.R. Williams, 1998. Large Area Hydrologic Modeling and Assessment: Part I. Model Development. Journal of American Water Resources Association 34:73-89.

Cayan, D.R., M.D. Dettinger, H.F. Diaz, and N.E. Graham, 1998. Decadal Variability of Precipitation Over Western North America. Journal of Climate 11:3148-3166.

Gerbert, W.A., D.J. Graczyk, and W.R. Krug, 1987. Average Annual Runoff in the United States, 1951-80. U.S. Geological Survey, Reston, Virginia.

Gleick, P.H., 1990. Climate Change and U.S. Water Resources. *In:* Vulnerability of Water Systems, P.E. Waggoner (Editor). Wiley Interscience, New York, pp. 223-240.

Gu, D. and S.G.H. Philander, 1995. Secular Changes of Annual and Interannual Variability in the Tropics During the Past Century. Journal of Climate 8:864-876.

Guetter, A.K. and K.P. Georgakakos, 1993. River Outflow of the Conterminous United States 1939-1988. Bulletin of the American Meteorological Society 74:1873-1891.

Hastenrath, S., 1990. Decadal-Scale Changes of the Circulation in the Tropical Atlantic Sector Associated With Sahel Drought. International Journal of Climatology 10:459-472.

Houghton, R.W. and Y.M. Tourre, 1992. Characteristics of Low Frequency Sea Surface Temperature Fluctuations in the Tropical Atlantic. Journal of Climate 5:765-771.

Hurrell, J.W., Y. Kushnir, and M. Visbeck, 2001. The North Atlantic Oscillation. Science 291:603-605.

Kestin, T.S., D.J. Karoly, and J.-I. Yano, 1998. Time-Frequency Variability of ENSO and Stochastic Simulations. Journal of Climate 11:2258-2272.

Lins, H.F., 1997. Regional Streamflow Regimes and Hydroclimatology of the United States. Water Resources Research 33:1655-1667.

Mantua, N.J., S.R. Hare, Y. Zhang, J.M. Wallace, and R.C. Francis, 1997. A Pacific Decadal Climate Oscillation With Impacts on Salmon. Bulletin of the American Meteorological Society 78:1069-1079.

Mather, J.R., 1984. Water Resources: Distribution, Use, and Management. Wiley Interscience, New York.

Maurer, E.P., A.W. Wood, J.C. Adam, and D.P. Lettenmaier, 2002. A Long-Term Hydrologically Based Dataset of Land Surface Fluxes and States for the Conterminous United States. Journal of Climate 15:3237-3251.

McCabe, G.J. and M.D. Dettinger, 1999. Decadal Variations in the Strength of ENSO Teleconnections With Precipitation in the Western United States. International Journal of Climatology 19:1399-1410.

Mehta, V.M., 1998. Variability of the Tropical Ocean Surface Temperatures at Decadal-Multidecadal Timescaes, Part I: The Atlantic Ocean. Journal of Climate 11:2351-2375.

Mehta, V.M. and T. Delworth, 1995. Decadal Variability of the Tropical Atlantic Ocean Surface Temperature in Shipboard Measurements and in a Global Ocean-Atmosphere Model. Journal of Climate 8:172-190.

Mehta, V.M. and K.-M. Lau, 1997. Influence of Solar Irradiance on the Indian Monsoon-ENSO Relationship at Decadal-Multidecadal Time Scales. Geophysical Research Letters 24:159-162.

Murray, S., 2005. Drought Along the Missouri Divides the Senate. The Washington Post, July 5.

OSTP (Office of Science and Technology Policy, Executive Office of the President), 2000. Climate Change Impacts on the United States: The Potential Consequences of Climate Variability and Change.

Power, S., T. Casey, C. Folland, A. Colman, and V.M. Mehta, 1999. Interdecadal Modulation of the Impact of ENSO on Australia. Climate Dynamics 15:319-324.

Press, W.H., S.A. Teukolsky, W.T. Vetterling, and B.P. Flannery, 2001. Numerical Receipes: The Art of Scientific Computing. Cambridge University Press, New York.

Rajagopalan, B., Y. Kushnir, and Y.M. Tourre, 1998. Observed Decadal Midlatitude and Tropical Atlantic Climate Variability. Geophysical Research Letters 25:3967-3970.

Rasmusson, E.M., 1991. Observational Aspects of ENSO Cycle Teleconnections. *In*: Teleconnections Linking Worldwide Climate Anomalies, M.H. Glantz, R.W. Katz, and N. Nichols (Editors). Cambridge University Press, Cambridge, pp. 309-343.

Richardson, C.W. and A.D. Nicks, 1990. Weather Generator Description. *In:* EPIC-Erosion Productivity Impact Calculator: I. Model Documentation. A.N. Saharpley and J.R. Williams (Editors). U.S. Department of Agriculture Technical Bulletin No. 1768.

Ropelewski, C. and M. Halpert, 1986. North American Precipitation and Temperature Patterns Associated With the El Niño/Southern Oscillation (ENSO). Monthly Weather Review 114:2352-2362.

Rosenberg, N.J., 1993. Towards an Integrated Impact Assessment of Climate Change: The MINK Study. Climatic Change 24: 1-173.

Rosenberg, N.J., 2007. A Biomass Future for the North American Great Plains. Springer, Dordrecht, The Netherlands.

Rosenberg, N.J., R.A. Brown, R.C. Izaurralde, and A.M. Thomson, 2003. Integrated Assessment of Hadley Centre Climate Change Projections on Water Resources and Agricultural Productivity in the Conterminous United States. I. Climate Change Scenarios and Impacts on Water Resources Simulated With the HUMUS Model. Agricultural Forestry and Meteorology 117:73-96.

Smith, S.R., D.M. Legler, M.J. Remigio, and J.J. O'Brien, 1999. Comparison of 1997-98 U.S. Temperature and Precipitation Anomalies to Historical ENSO Warm Phases. Journal of Climate 12:3507-3515.

Srinivasan, R., J.G. Arnold, R.S. Muttiah, C. Walker, and P.T. Dyke, 1993. Hydrologic Unit Model for the United States (HUMUS). Advances in Hydroscience and Engineering. CCHE, University of Mississippi, Oxford, Mississippi.

Stockle, C.O., P.T. Dyke, J.R. Williams, C.A. Jones, and N.J. Rosenberg, 1992a. Estimation of the Effects of CO_2-Induced Climate Change on Growth and Yield of Crops. II. Assessing the Impacts on Maize, Wheat and Soybean in the Midwestern USA. Agricultural Systems 38:239-256.

Stockle, C.O., J.R. Williams, N.J. Rosenberg, and C.A. Jones, 1992b. Estimation of the Effects of CO_2-Induced Climate Change on Growth and Yield of Crops. I. Modification of the EPIC Model for Climate Change Analysis. Agricultural Systems 38:225-238.

Thomson, A.M., R.A. Brown, N.J. Rosenberg, R.C. Izaurralde, D.M. Legler, and R. Srinivasan, 2003. Simulated Impacts of El Nino/Southern Oscillation on U.S. Water Resources. Journal of American Water Resources Association 39:137-148.

Thomson, A.M., R.A. Brown, N.J. Rosenberg, R. Srinivasan, and R.C. Izaurralde, 2005a. Climate Change Impacts for the Conterminous USA: An Integrated Assessment, Paper 4, Water Resources. Climatic Change 69:67-88.

Thomson, A.M., N.J. Rosenberg, R.C. Izaurralde, and R.A. Brown, 2005b. Models and Validation. Part II in N.J. Rosenberg and J.A. Edmonds, eds. Climate Change Impacts for the Conterminous USA. Climatic Change 69:27-41.

Thomson, A.M., N.J. Rosenberg, R.C. Izaurralde, and R.A. Brown, 2005c. Climate Change Impacts for the Conterminous USA: An Integrated Assessment, Paper 5, Irrigated Agriculture and National Grain Crop Production. Climatic Change 69:89-105.

Ting, M. and H. Wang, 1997. Summertime U.S. Precipitation Variability and Its Relation to Pacific Sea Surface Temperature. Journal of Climate 10:1853-1873.

Torrence, C. and P.J. Webster, 1999. Interdecadal Changes in the ENSO-Monsoon System. Journal of Climate 12:2679-2690.

USGS, 1987. Hydrologic Unit Maps (Rep. No.2294). US Government Printing Office, Washington, D.C.

Waggoner, P.E. and J. Shefter, 1990. Climate Change and U.S. Water Resources. *In:* Future Water Use in the Present Climate, P.E. Waggoner (Editor). Wiley, New York, pp. 19-39.

Wang, H. and V.M. Mehta, 2008. Decadal Variability of the Indo-Pacific Warm Pool and Its Association With Atmospheric and Oceanic Variability in the NCEP-NCAR and SODA Reanalyses. Journal of Climate 21:5545-5565.